

PET Network Abnormalities and Cognitive Decline in Patients with Mild Cognitive Impairment

Davangere P Devanand^{*1,2,4}, Christian G Habeck^{2,4}, Matthias H Tabert^{1,4}, Nikolaos Scarmeas^{2,4}, Gregory H Pelton^{1,2,4}, James R Moeller¹, Brett D Mensh¹, Tyler Tarabula¹, Ronald L Van Heertum³ and Yaakov Stern^{2,4}

¹Department of Biological Psychiatry, College of Physicians and Surgeons, New York State Psychiatric Institute, Columbia University, New York, NY, USA; ²Department of Neurology, College of Physicians and Surgeons, Gertrude H. Sergievsky Center, Columbia University, New York, NY, USA; ³Department of Radiology, College of Physicians and Surgeons, Gertrude H. Sergievsky Center, Columbia University, New York, NY, USA; ⁴Taub Institute for Research in Alzheimer's Disease and the Aging Brain, Columbia University, New York, NY, USA

Temporoparietal and posterior cingulate metabolism deficits characterize patients with Alzheimer's disease (AD). A H₂¹⁵O resting PET scan covariance pattern, derived by using multivariate techniques, was previously shown to discriminate 17 mild AD patients from 16 healthy controls. This AD covariance pattern revealed hypoperfusion in bilateral inferior parietal lobule and cingulate; and left middle frontal, inferior frontal, precentral, and supramarginal gyri. The AD pattern also revealed hyperperfusion in bilateral insula, lingual gyri, and cuneus; left fusiform and superior occipital gyri; and right parahippocampal gyrus and pulvinar. In an independent sample of 23 outpatients with mild cognitive impairment (MCI) followed at 6-month intervals, the AD pattern score was evaluated as a predictor of cognitive decline. In this MCI sample, an H₂¹⁵O resting PET scan was carried out at baseline. Mean duration of follow-up was 48.8 (SD 15.5) months, during which time six of 23 MCI patients converted to AD. In generalized estimating equations (GEE) analyses, controlling for age, sex, education, and baseline neuropsychological scores, increased AD pattern score was associated with greater decline in each neuropsychological test score over time (Mini Mental State Exam, Selective Reminding Test delayed recall, Animal Naming, WAIS-R digit symbol; *P*s < 0.01–0.001). In summary, a resting PET covariance pattern previously reported to discriminate AD patients from control subjects was applied prospectively to an independent sample of MCI patients and found to predict cognitive decline. Independent replication in larger samples is needed before clinical application can be considered.

Neuropsychopharmacology (2006) **31**, 1327–1334. doi:10.1038/sj.npp.1300942; published online 9 November 2005

Keywords: PET; mild cognitive impairment; Alzheimer's disease; network abnormalities

INTRODUCTION

Regional cerebral blood flow (rCBF) and metabolism (rCMRglc) deficits, primarily in the temporoparietal and posterior cingulate regions, are early features of Alzheimer's disease (AD). Decreased rCBF and rCMRglc may represent metabolic insufficiency prior to neuronal loss, may be secondary to local neuronal loss, or may reflect amyloid-related vascular pathology in the walls of blood vessels (Gsell *et al*, 2000; Cummings, 2004). Another contributing factor may be the loss of cholinergic projections from the basal forebrain to the hippocampus and neocortex.

*Correspondence: Dr DP Devanand, Department of Biological Psychiatry, New York State Psychiatric Institute, 1051 Riverside Drive, Unit 126, New York, NY 10032, USA, Tel: +1 212 543 5612, Fax: +1 212 543 5088, E-mail: dpd3@columbia.edu
Received 15 July 2005; revised 19 August 2005; accepted 13 September 2005

Online publication: 14 September 2005 at <http://www.acnp.org/citations/Npp091405050459/default.pdf>

Temporoparietal metabolism deficits characteristically distinguish AD from controls, with high sensitivity (around 90% across studies) but only moderate specificity (Hoffman *et al*, 2000; Silverman *et al*, 2001; Herholz *et al*, 2002). Most of these studies included patients with moderate to severe AD, and predictive accuracy may not be as high in mild AD (Ishii *et al*, 1997; Herholz *et al*, 1999; De Santi *et al*, 2001). Nonetheless, expert clinical reading of PET may improve diagnostic accuracy for AD with reductions in false negatives and false positives (Silverman *et al*, 2001, 2002). In addition to temporoparietal deficits, posterior cingulate hypometabolism, which may reflect compromised projections from medial temporal regions, may characterize AD (Auppee *et al*, 2001; Millien *et al*, 2002).

The utility of these rCBF and rCMRglc deficits in predicting cognitive decline in cognitively impaired, non-demented patients is not established (Minoshima *et al*, 1997; Arnaiz *et al*, 2001; Huang *et al*, 2002). Cognitive processes generally reflect activity across brain networks rather than discrete regions in isolation, and this functional

connectivity can be evaluated by multivariate methods (Alexander and Moeller, 1994; Friston, 1994). Using resting $H_2^{15}O$ PET, we reported that a multivariate technique (Scaled Subprofile Modeling or SSM) that examines covariance patterns to identify alterations in network expression successfully discriminated mild AD patients from healthy control subjects ($p = 0.03$; sensitivity 76%, specificity 81% at the optimal cut-point for the covariance pattern), whereas SPM and ROI analyses did not show significant differences (Scarmeas *et al*, 2004). The previously identified covariance pattern showed negative loadings (hypoperfusion) in bilateral inferior parietal lobule and cingulate; and left middle frontal, inferior frontal, precentral and supramarginal gyri. Positive loadings (hyperperfusion) were seen in bilateral insula, lingual gyri, and cuneus; left fusiform and superior occipital gyri; and right parahippocampal gyrus and pulvinar. The mean pattern expression was significantly greater in AD patients compared to controls, even after controlling for age.

In the same report, we described resting $H_2^{15}O$ PET results in outpatients with mild cognitive impairment (MCI), who presented with memory complaints and demonstrated cognitive deficits on neuropsychological testing. In the MCI sample examined cross-sectionally, the identified covariance pattern (AD pattern) differentiated patients with baseline Clinical Dementia Rating (CDR) 0 from patients with baseline CDR 0.5 (questionable dementia), and it inversely correlated with neuropsychological measures (Scarmeas *et al*, 2004). In this longitudinal study, we hypothesized that forward application of the previously identified AD pattern would predict cognitive decline over time in the MCI sample.

MATERIALS AND METHODS

Subjects

Patients who presented with memory complaints to a Memory Disorders Center participated in a longitudinal study of putative early diagnostic markers of AD. The research protocol was approved by the New York State Psychiatric Institute and Columbia Presbyterian Medical Center IRBs, and written informed consent was obtained.

For patients, inclusion criteria were age ≥ 40 years, intellectual impairment ≥ 6 months and ≤ 10 years, and the diagnosis of 'not demented' (CDR = 0) or 'questionably demented' (CDR = 0.5). Patients had a minimum modified mMMSE score ≥ 40 out of 57 (Folstein MMSE ≥ 22). Neuropsychological testing screening guidelines were recall ≤ 2 out of three objects at 5 min on the Mini Mental State Exam (MMSE), or a delayed recall score > 1 SD below norms on the Selective Reminding Test (SRT), or a Wechsler Adult Intelligence Scale-Revised (WAIS-R) performance IQ score ≥ 10 points below the WAIS-R verbal IQ score (Devanand *et al*, 2000; Tabert *et al*, 2002). Patients without any of these deficits were eligible if they met all the following criteria: subjective complaint of memory decline, informant's confirmation of decline, and a positive score on at least one of the first eight items of the modified Blessed Functional Activity Scale (Devanand *et al*, 2005).

Exclusion criteria were a diagnosis of dementia, schizophrenia, schizoaffective disorder, or primary major affective

disorder, electroconvulsive therapy within the past 6 months, current or recent (past 6 months) history of alcohol or substance dependence (DSM-IV criteria), clinical or historical evidence of stroke, cortical stroke or an infarct ≥ 2 cm in diameter on any MRI slice, cognitive impairment rated as entirely caused by concomitant medications, and major neurological illness.

Patients who met these inclusion/exclusion criteria were defined as having MCI and were followed at 6-month intervals (Devanand *et al*, 2005). The physician's assessment, Folstein MMSE, and SRT were completed at each 6-month interval, with the entire neuropsychological test battery administered at annual visits.

Procedures

The study physician (neurologist or psychiatrist) completed a medical history and conducted a general physical, neurological, and psychiatric examination. Laboratory tests included complete blood count with differential, serum electrolytes, liver and renal function tests, thyroid function tests, VDRL, serum B12 and folate levels, and brain MRI scan. A trained neuropsychology technician administered the following tests: WAIS-R, Wechsler Memory Scale (WMS), SRT (12-item), Rosen Drawing Test, Controlled Oral Word Association, category naming from the Boston Diagnostic Aphasia Evaluation, Boston Naming Test, Benton Visual Retention Test, and Target Finding (shape and letter cancellation tasks). The analyses of neuropsychological variables were restricted *a priori* to the Folstein MMSE and single measures of verbal memory (SRT delayed recall), verbal fluency (Animal Naming), and attention/executive function (WAIS-R digit symbol), which are well-established predictors of MCI conversion to AD (Jacobs *et al*, 1995; Devanand *et al*, 2005).

The neuropsychological scores were evaluated by an experienced neuropsychologist (YS), and two expert clinical raters (DPD and YS) used these results, clinical and laboratory test results, and MRI clinical reads to make a consensus research diagnosis at all visits (Devanand *et al*, 2000, 2005; Tabert *et al*, 2002). The diagnosis of dementia was based on DSM-IV criteria, and the diagnosis of possible or probable AD was based on NINCDS-ADRDA criteria (McKhann *et al*, 1984). PET results did not play any role in the diagnostic process. Apolipoprotein E genotype was assessed in all subjects (Hixson and Powers, 1991), and patients were characterized as $\epsilon 4$ carriers ($\epsilon 3/\epsilon 4$ or $\epsilon 2/\epsilon 4$ or $\epsilon 4/\epsilon 4$) or $\epsilon 4$ noncarriers.

PET Scan Acquisition and Processing

A Siemens EXACT 47 PET camera (Knoxville, TN, USA) was used to acquire resting $H_2^{15}O$ PET scans. A bolus of 30 mCi $H_2^{15}O$ was injected intravenously. Scan acquisition was triggered by the detection of a threshold level of true counts from the camera. Two 30-s scan frames were acquired in 2-D mode, which were subsequently averaged to yield a single image per subject. After measured attenuation correction (15-min transmission scan) and reconstruction by filtered back-projection, image resolution was 4.6 mm full-width at half-maximum (FWHM). Arterial blood sampling was not conducted, thus only nonquantitative count images (and

not absolute rCBF measures) were obtained. Each subject's image was spatially transformed to the PET Montreal Neurological Institute brain space template included with the SPM99 program (Wellcome Department of Neurology). The spatially transformed images were smoothed with an isotropic, Gaussian kernel (FWHM = 12 mm).

Covariance Analysis

The spatial covariance analytic method, SSM, is a form of principal component analysis that captures regionally correlated local percent changes from the mean voxel activity of a reference subject group, without contamination by subject differences in global blood flow (Alexander and Moeller, 1994; Moeller *et al*, 1987). This method has been used to distinguish the blood flow pattern (and metabolism pattern using FDG PET) in patients with specific neurological and psychiatric disorders from the pattern observed in normal control subjects (Eidelberg *et al*, 1998; Stern *et al*, 2000; Su *et al*, 2001).

We reported on the derivation of a covariance analysis-based blood flow pattern that distinguished AD patients from healthy controls, as described elsewhere in detail (Scarmeas *et al*, 2004). In this longitudinal study, the previously derived AD covariance pattern was prospectively applied to the PET perfusion data in the independent sample of 23 MCI patients. The operation of forward application was represented mathematically by a 'dot' product computation: every voxel value in a subject scan was multiplied by the corresponding voxel weight in the AD pattern, with a subsequent summation over the whole brain volume to derive the subject scaling factor, or SSF, for the subject. This SSF factor quantifies the degree of AD pattern expression in each subject's PET scan; we refer to the AD pattern score as the SSF. The SSF was tested as a predictor of cognitive decline in the MCI sample.

ROI Analyses

T1-weighted anatomical MRI scans from eight elderly healthy control subjects (mean age 67.3, SD 4.2 years, 75% male, no neurological or psychiatric disorder, no cognitive impairment) were acquired axially on a 1.5-T GE scanner (1.5-mm slice thickness, 0.86-mm in-plane resolution, TE = 5 ms, TR = 34 ms). The MRIs were reoriented coronally, AC-PC aligned and then segmented and parcellated into 130 regions (96 of them cortical gray matter) using the Cardviews software program (Goldstein *et al*, 1999). A single rater, who had been formally trained by the Cardviews group, labeled each region in a semiautomated manner using a combination of hand-drawing with a cursor and local thresholding with a histogram. The labeled brains were spatially normalized into MNI space (FLIRT from FSL, developed by FMRIB, Oxford, <http://www.fmrib.ox.ac.uk>). A probabilistic atlas in this standard space was constructed by allowing each atlas brain to contribute equally to the region identity for each voxel. For example, at Talairach [4, 34, 38], 6/8 report 'Right Posterior Cingulate Gyrus' and 2/8 report 'Right White Matter', so the probabilities assigned to those two regions at that voxel are 0.75 and 0.25, respectively. The PET images were registered to this space and the regional CBF was determined by taking a weighted

average of the CBF voxel values over each probabilistically defined region. ROI analyses were conducted for three regions (sum of right and left) selected *a priori* based on the literature: hippocampus, parahippocampus, and posterior cingulate (Ishii *et al*, 1997; Herholz *et al*, 1999, 2002; De Santi *et al*, 2001), followed by exploratory ROI analyses for all 130 regions.

Statistics

Two-tailed *t*-test and χ^2 test (or Fisher's exact test) were used to compare the features of patients and controls. We used generalized estimating equations (GEE) to test whether the AD pattern score (SSF) was associated with differential rates of cognitive decline (Liang and Zeger, 1986). GEE takes into account the multiple visits per subject and the fact that the characteristics of the same subject over time are likely to be correlated. The repeated measures for each subject are treated as a cluster. The GEE model included each of four neuropsychological scores as the dependent variable and, as predictors, the AD pattern score (SSF), time (years from baseline assessment), and an SSF \times time interaction. GEE models were additionally adjusted for baseline age, sex, education, and baseline neuropsychological scores.

Conversion to AD was defined as meeting clinical diagnostic criteria for probable AD at two consecutive assessments (6-month intervals). Only six patients converted to AD, so the analyses for prediction of conversion to AD were considered exploratory. Since follow-up duration varied across subjects, Cox proportional hazards models were used to examine the effect of the previously identified AD pattern score (SSF) on the development of AD, controlling for sex, baseline age, education and baseline MMSE scores. The time variable was the initial visit to the first follow-up time-point at which AD was diagnosed. An ROC curve was plotted to determine the optimal AD pattern score (SSF) for prediction of the follow-up diagnosis of AD. Similar GEE and Cox analyses were conducted for the ROIs, focusing on the three ROI measures selected *a priori*.

RESULTS

Sample Characteristics

The demographic and clinical features of the sample are described in Table 1. Mean duration of follow-up was 48.8 (SD 15.5) months with an average of 8 (SD 2.3) assessments per subject. Converters to AD reached their conversion time-point an average of 42 (SD 15.2) months after the initial evaluation. Nonconverters ($n = 17$) were followed for an average of 51.2 (SD 15.3) months. Converters to AD during follow-up ($n = 6$) were older than the 17 nonconverters, and had lower baseline MMSE, SRT delayed recall, and WAIS-R digit symbol scores (Table 1).

AD Covariance Pattern (SSF)

The AD pattern score (SSF) showed a trend-level correlation with age ($r = 0.37$, $p = 0.08$) but was not associated with sex or education.

In the MCI sample ($n = 23$), GEE analyses were conducted on the time trend in MMSE, SRT delayed recall, Animal

Table 1 Baseline Features of Converters and Nonconverters to AD

Feature	Converters (n = 6)	Nonconverters (n = 17)	^a p <
Sex, %F	26	74	0.06
Age in years, mean ± SD	75.0 ± 4.9	65.8 ± 9.7	0.04
Education in years, mean ± SD	17.8 ± 1.6	16.4 ± 2.2	0.16
<i>Ethnic group</i>			
Whites (%)	100	88.2	0.6
Hispanics (%)	0	5.9	—
Blacks (%)	0	0	—
Other (%)	0	5.9	—
MMSE, mean ± SD	27.2 ± 0.36	29.0 ± 0.94	0.001
SRT delayed recall, mean ± SD	2.7 ± 1.9	6.9 ± 3.3	0.01
Animal naming, mean ± SD	19.1 ± 5.9	20.3 ± 5.2	0.67
WAIS-R digit symbol, mean ± SD	38.0 ± 6.9	49.8 ± 12.2	0.04
Apolipoprotein E ε4 carrier	66.7%	23.5%	0.09
Subject Scaling Factor (SSF)	26.4 ± 5.7	21.9 ± 5.7	0.12

^aA test of significance (p = probability) for χ^2 or Fisher's exact test (categorical variables) or two-tailed t -test (continuous variables), conducted as appropriate. MMSE: 30-item Mini-Mental State Exam; SRT: Selective Reminding Test of Buschke and Fuld; WAIS-R: Wechsler Adult Intelligence Scale-Revised; SSF: Subject Scaling Factor, or AD pattern expression.

Naming and WAIS-R digit symbol scores, respectively. For the linear time trend in MMSE, after controlling for age, sex, education, and baseline MMSE, there was a significant time effect ($p < 0.02$), and a significant SSF (AD pattern score) by time interaction ($p < 0.002$; Figure 1). More robust results were obtained for the other three neuropsychological measures in similar GEE analyses with the same covariates. For SRT delayed recall, there was a significant time effect ($p < 0.0001$) and a significant SSF by time interaction ($p < 0.0001$). For animal naming, there was a significant time effect ($p < 0.0001$) and a significant SSF by time interaction ($p < 0.0001$). For WAIS-R digit symbol, there was a significant time effect ($p < 0.001$) and a significant SSF by time interaction ($p < 0.001$).

In the MCI sample, the AD pattern score (SSF) tended to be associated with the follow-up diagnosis of AD ($p = 0.1$). Figure 2 illustrates the scatter-plot of the SSF values in the MCI converters and nonconverters to AD, and in the previously reported AD ($n = 17$) and healthy control ($n = 16$) groups (Scarmeas et al, 2004). Based on an ROC curve, the optimal SSF value was 23, which was nearly identical to the sample median (22.8) and led to a sensitivity of 83.3% and specificity of 58.8% for prediction of the follow-up diagnosis of AD. The area under the ROC curve (AUC) was 0.735. Since only six patients converted to AD, Cox proportional hazards model analyses were exploratory. In these analyses, the SSF was not a significant predictor of conversion to AD ($p < 0.17$), and neither was the SSF dichotomized around the optimal value based on the ROC curve (SSF = 23; risk ratio = 5.3, 95% CI 0.6–45.8, $p = 0.13$).

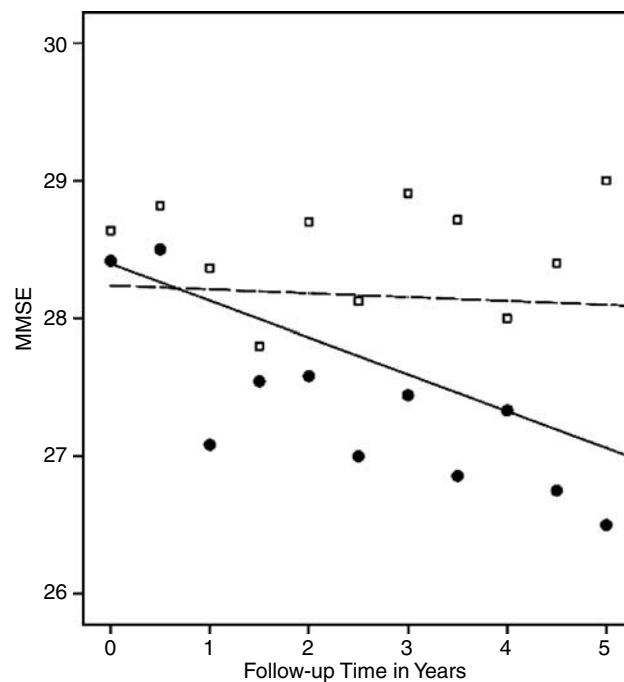


Figure 1 Summary of generalized estimating equations (GEE) analyses on the effect of the baseline covariance pattern (SSF, dichotomized around median score 23) on change in Mini Mental State Exam (MMSE) over time, controlling for age, sex, education and baseline MMSE. For patients with high SSF expression, open squares represent the mean MMSE values at each visit used in the GEE analyses, and for patients with low SSF expression, solid circles represent the mean MMSE values at each visit. The corresponding regression lines (broken line for high SSF and solid line for low SSF) have been constructed using the GEE-derived predicted MMSE values.

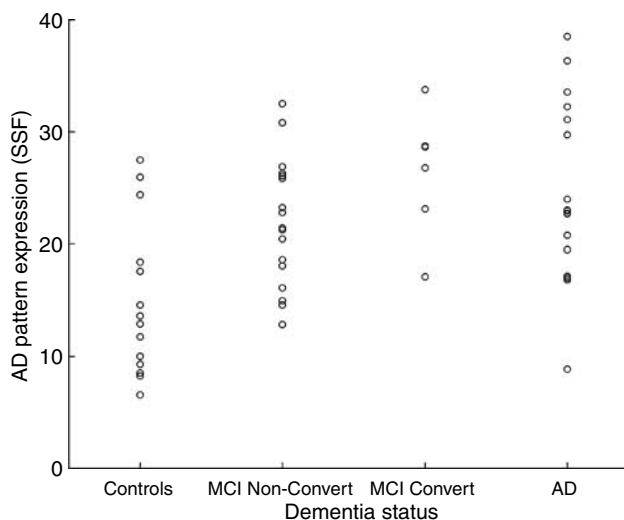


Figure 2 AD pattern expression values (SSF) in 16 healthy control subjects, 17 MCI nonconverters to AD, six MCI converters to AD, and 17 AD patients.

ROI Analyses

ROI analyses were conducted for three *a priori* regions (sum of right and left): hippocampus, parahippocampus, and posterior cingulate. In univariate analyses, among these three ROIs, only flow reduction in the posterior cingulate

predicted conversion to AD ($p < 0.05$, two-tailed t -test, corrected for three comparisons). In a Cox proportional hazards model, the posterior cingulate was not a significant predictor of conversion to AD ($p < 0.15$), and it remained nonsignificant ($p < 0.3$) after controlling for age, sex, education, and baseline MMSE. In similar Cox analyses, neither the hippocampus nor the parahippocampus ROI was significant.

Next, we computed the average blood flow in 130 gray and white-matter ROIs and proportionally scaled them by the whole-brain flow value. In exploratory univariate analyses (two-tailed t -tests), only two brain regions showed lower values for converters compared to nonconverters (right and left posterior cingulate, $p < 0.05$), which became nonsignificant after correcting for multiple comparisons.

In GEE analyses, controlling for age, sex, education, and corresponding baseline neuropsychological score, there was no significant posterior cingulate (sum of right and left) by time interaction on the time trend in MMSE or SRT delayed recall or WAIS-R digit symbol scores. In comparable GEE analyses, there was a significant posterior cingulate by time interaction on the time trend in Animal Naming ($p < 0.02$). In similar GEE analyses on the same neuropsychological variables using the same covariates, there were no significant hippocampus by time or parahippocampus by time interactions.

Apolipoprotein E $\epsilon 4$ Allele

Among the six converters to AD, four (66.7%) were $\epsilon 4$ carriers (two heterozygous and two homozygous) compared to four of 17 (23.5%) $\epsilon 4$ carriers (all heterozygous) among nonconverters to AD (Fisher's exact test, $p < 0.14$). Three of six (50%) $\epsilon 4$ carriers with high SSF scores (> 23) converted to AD, compared to two of 15 (11.8%) converters in the rest of the sample (Fisher's exact test, $p < 0.09$). In a Cox model, patients who were $\epsilon 4$ carriers with high AD pattern expression (SSF > 23) tended to be more likely to convert to AD than the rest of the sample (risk ratio 4.2, 95% CI 0.9–21, $p < 0.08$), but this effect became nonsignificant after controlling for age, sex, education and baseline MMSE.

DISCUSSION

In our recent report, multivariate analysis was superior to univariate methods in discriminating mild AD from controls, and in the MCI sample, patients with CDR 0 differed in their AD pattern scores from patients with CDR 0.5 (Scarmeas *et al*, 2004). In this longitudinally studied MCI sample, in GEE analyses for all four neuropsychological measures, this AD pattern score was associated with greater cognitive decline over time even after controlling for age, sex, education, and baseline cognitive test performance. This result indicates the unique strength of this study, in that a covariance pattern that was empirically derived as discriminating AD patients from control subjects was then forward-applied to an independent sample of MCI patients and found to have predictive utility for cognitive decline during follow-up, even after controlling for relevant demographic variables and baseline cognitive scores.

Other investigators have utilized multivariate analytic techniques to distinguish AD from control subjects (Azari *et al*, 1993; Grady *et al*, 2001) and to predict conversion to AD (Johnson *et al*, 1998). In a Tc-HMPAO SPECT study, the pattern derived from multivariate analysis showed 84.4% accuracy in discriminating 27 questionable dementia patients who did not progress from 18 questionable dementia subjects who converted to AD during 2 years of follow-up (Johnson *et al*, 1998). Less information is available on the utility of PET abnormalities in predicting cognitive decline in healthy control subjects. Using traditional analytic techniques, de Leon *et al* (2001) showed that reduction in entorhinal glucose metabolism (FDG PET) was associated with cognitive decline in a sample of 48 normal elderly subjects followed for 3 years, with entorhinal metabolism correctly classifying cognitive decline with 84% accuracy.

In exploratory Cox survival analyses, we found that the AD pattern score was not a significant predictor of conversion to AD. The risk ratio was fairly high (5.3 without controlling for other variables), but the variability led to wide confidence intervals and reduction in significance in this small sample. Two nonconverters expressed the AD pattern to a marked degree: one of them has begun to show cognitive decline after 4 years of follow-up and another is cognitively stable. Both subjects are apoE $\epsilon 4$ carriers, and high AD pattern scores in $\epsilon 4$ carriers tended to be associated with an increased risk of conversion to AD, consistent with other reports that used different analytic techniques (Small *et al*, 1995; Reiman *et al*, 1996). Other PET reports in MCI (or similar) samples followed longitudinally have also involved small numbers of subjects, and have generally utilized univariate techniques. In 20 MCI patients followed for an average of 3 years, the strongest predictors of AD were decreased rCMRglu from the left temporoparietal area and impaired performance on block design (Arnaiz *et al*, 2001). In other studies of small samples of MCI patients followed for up to 2 years, lower temporoparietal FDG uptake or posterior cingulate hypometabolism characterized conversion to AD (Chetelat *et al*, 2003; Drzezga *et al*, 2003). In another FDG PET study, posterior cingulate but not temporoparietal hypometabolism predicted conversion to AD during 4–39 months of follow-up (Minoshima *et al*, 1997). In 54 MCI patients followed for 2 years, Tc-HMPAO SPECT showed decreased left posterior cingulate blood flow in decliners compared to nondecliners (Huang *et al*, 2002). Earlier FDG PET work in AD patients suggested that neocortical abnormalities may precede impairment of abstract reasoning and attention by 8–16 months (Grady *et al*, 1988).

In our recent report, we showed that the covariance analytic method (SSM), but not traditional ROI analyses, distinguished AD patients from control subjects (Scarmeas *et al*, 2004). In ROI analyses in this longitudinal MCI study, the posterior cingulate (flow reduction) was the only region that predicted AD. However, it was not significant after correcting for multiple comparisons, it was not significant in Cox analyses, and its interaction with time was not significant in most of the GEE analyses. These results suggest that traditional ROI analyses were not as sensitive as SSM, which was sensitive to cognitive decline for all the neuropsychological measures examined in the GEE

analyses. One caveat is that the atlas-based normalization approach may not adequately capture hippocampal regions because of spatial distortion, thus decreasing the sensitivity of the ROI analysis for this region (Mosconi *et al*, 2005). Further, it is not known if the SSM approach is superior to other methods with potential utility in predicting cognitive decline and conversion to AD in MCI patients, for example, resting FDG PET (Silverman *et al*, 2002), hippocampal and entorhinal atrophy on structural MRI (de Leon *et al*, 2004), CSF tau and A-Beta levels (Blennow and Vanmechelen, 2003). Head-to-head comparison of these measures in larger samples of MCI patients followed longitudinally is needed to address this issue.

Cognitive activation paradigms using PET may improve sensitivity, particularly in distinguishing AD from controls (Stern *et al*, 2000; Grady *et al*, 2001; Horwitz *et al*, 1995). However, in MCI patients, predictive utility for cognitive activation paradigms is not established, and clinical applicability is more limited than for resting PET.

There were several limitations to this study. H₂¹⁵O PET is noisier and has lower resolution than FDG PET (Wu *et al*, 2003). The degree to which cerebral blood flow is coupled to cerebral metabolism remains controversial (Mintun *et al*, 2001), and it is unclear if this coupling is maintained in MCI and AD. In our MCI sample, the exclusion of subjects with stroke and significant cerebrovascular disease suggests that vascular pathology is an unlikely explanation for the findings. Arterial blood was not sampled to provide absolute quantification, partly due to practical limitations and partly to make the PET procedure comparable to general clinical usage. In several cases, MRI was not conducted in temporal proximity to the PET scan, and hence partial volume correction for atrophy could not be done. The latter has a small but sometimes material effect in the interpretation of PET data in distinguishing AD patients from controls (Tanna *et al*, 1991; Meltzer *et al*, 1996). Our sample size was small, thereby reducing statistical power. However, the technique was powerful enough to demonstrate significant effects on rates of change over time. Another caveat is that the clinical diagnosis of AD is not always accurate and could have led to error in diagnostic outcome classification during follow-up. This issue was partly addressed by the use of systematic diagnostic methods and the evaluation of change over time in cognitive performance (GEE analyses) that diminished the potential bias in diagnostic assessment.

The damage that occurs in AD likely affects connections in brain networks and is not restricted to the hippocampus or entorhinal cortex. The covariance pattern that discriminated AD from controls also predicted cognitive decline with forward application to an independent sample of MCI patients, indicating that the expression of this AD pattern is likely related to the disease process itself. Areas showing decreased flow in the pattern included the cingulate, inferior parietal lobule, and supramarginal gyrus, but the parahippocampal region showed increased flow in this pattern. As we previously suggested (Scarmeas *et al*, 2004), it is possible that reduced flow because of AD pathology in certain nodes of the pattern (cingulate, inferior parietal lobule, and supramarginal gyrus) may affect the whole pattern and lead to increased flow in another node in the pattern (parahippocampal gyrus). This speculation is

supported by an MRI arterial spin labeling study showing that hippocampal rCBF increased in very mild AD but then gradually subsided as AD became more severe (Press *et al*, 2003), suggesting a possible compensatory hippocampal response in very early AD.

Several regions in the AD covariance pattern, including the posterior cingulate and inferior parietal lobule, are known to be affected in AD. Posterior cingulate/flow deficits have been shown in MCI and AD patients, even though this region is not directly affected in very early AD (Huang *et al*, 2002; Braak and Braak, 1991). However, there are afferent and efferent connections between the posterior cingulate and the medial temporal cortex. The posterior cingulate contributes to spatial orientation and spatial working memory that may lie in parietal association area 7 and the parahippocampal gyrus with spatially selective firing in layer II of the entorhinal cortex (Huang *et al*, 2002). Cortico-cortical disconnection between these regions may lead to reduced metabolism in the posterior cingulate.

In summary, the covariance pattern previously shown to discriminate AD from controls was shown to have predictive utility for cognitive decline in an independent sample of MCI patients. This independently validated approach requires replication in large samples before clinical application can be considered.

ACKNOWLEDGEMENTS

This work was supported in part by a grant to Dr Devanand from the Alzheimer's Association and grants AG17761, MH55735, MH35636, MH55646, P50 AG08702.

REFERENCES

- Alexander GE, Moeller JR (1994). Application of the Scaled Subprofile Model to functional imaging in neuropsychiatric disorders: a principal component approach. *Hum Brain Mapp* 2: 79–94.
- Arnaiz E, Jelic V, Almkvist O, Wahlund LO, Winblad B, Valind S *et al* (2001). Impaired cerebral glucose metabolism and cognitive functioning predict deterioration in mild cognitive impairment. *Neuroreport* 12: 851–855.
- Aupee AM, Desgranges B, Eustache F, Lalevee C, de la Sayette V, Viader F *et al* (2001). Voxel-based mapping of brain hypometabolism in permanent amnesia with PET. *Neuroimage* 13: 1164–1173.
- Azari NP, Pettigrew KD, Schapiro MB, Haxby JV, Grady CL, Pietrini P *et al* (1993). Early detection of Alzheimer's disease: a statistical approach using positron emission tomographic data. *J Cereb Blood Flow Metab* 13: 438–447.
- Blennow K, Vanmechelen E (2003). CSF markers for pathogenic processes in Alzheimer's disease: diagnostic implications and use in clinical neurochemistry. *Brain Res Bull* 61: 235–242.
- Braak H, Braak E (1991). Neuropathological staging of Alzheimer-related changes. *Acta Neuropathol (Berl)* 82: 239–259.
- Chetelat G, Desgranges B, de la Sayette V, Viader F, Eustache F, Baron JC *et al* (2003). Mild cognitive impairment: can FDG-PET predict who is to rapidly convert to Alzheimer's disease? *Neurology* 60: 1374–1377.
- Cummings JL (2004). Alzheimer's disease. *N Engl J Med* 351: 56–67.
- de Leon MJ, Convit A, Wolf OT, Tarshish CY, DeSanti S, Rusinek H *et al* (2001). Prediction of cognitive decline in normal elderly subjects with 2-[¹⁸F]fluoro-2-deoxy-D-glucose/

- positron-emission tomography (FDG/PET). *Proc Natl Acad Sci USA* **98**: 10966–10971.
- de Leon MJ, DeSanti S, Zinkowski R, Mehta PD, Pratico D, Segal S et al (2004). MRI and CSF studies in the early diagnosis of Alzheimer's disease. *J Intern Med* **256**: 205–223.
- De Santi S, de Leon MJ, Rusinek H, Convit A, Tarshish CY, Roche A et al (2001). Hippocampal formation glucose metabolism and volume losses in MCI and AD. *Neurobiol Aging* **22**: 529–539.
- Devanand DP, Michaels-Marston KS, Liu X, Pelton GH, Padilla M, Marder K et al (2000). Olfactory deficits in patients with mild cognitive impairment predict Alzheimer's disease at follow-up. *Am J Psychiatry* **157**: 1399–1405.
- Devanand DP, Pelton GH, Zamora D, Liu X, Tabert M, Goodkind M et al (2005). Predictive utility of apolipoprotein E genotype for Alzheimer disease in outpatients with mild cognitive impairment. *Arch Neurol* **62**: 975–980.
- Drzezga A, Lautenschlager N, Siebner H, Riemenschneider M, Willoch F, Minoshima S et al (2003). Cerebral metabolic changes accompanying conversion of mild cognitive impairment into Alzheimer's disease: a PET follow-up study. *Eur J Nucl Med Mol Imaging* **30**: 1104–1113.
- Eidelberg D, Moeller JR, Antonini A, Kazumata K, Nakamura T, Dhawan V et al (1998). Functional brain networks in DYT1 dystonia. *Ann Neurol* **44**: 303–312.
- Friston KJ (1994). Functional and effective connectivity in neuroimaging: a synthesis. *Hum Brain Mapping* **2**: 56–78.
- Goldstein JM, Goodman JM, Seidman LJ, Kennedy DN, Makris N, Lee H et al (1999). Cortical abnormalities in schizophrenia identified by structural magnetic resonance imaging. *Arch Gen Psychiatry* **56**: 537–547.
- Grady CL, Furey ML, Pietrini P, Horwitz B, Rapoport SI (2001). Altered brain functional connectivity and impaired short-term memory in Alzheimer's disease. *Brain* **124**: 739–756.
- Grady CL, Haxby JV, Horwitz B, Sundaram M, Berg G, Schapiro M et al (1988). Longitudinal study of the early neuropsychological and cerebral metabolic changes in dementia of the Alzheimer type. *J Clin Exp Neuropsychol* **10**: 576–596.
- Gsell W, De Sadeleer C, Marchalant Y, MacKenzie ET, Schumann P, Dauphin F et al (2000). The use of cerebral blood flow as an index of neuronal activity in functional neuroimaging: experimental and pathophysiological considerations. *J Chem Neuroanat* **20**: 215–224.
- Herholz K, Nordberg A, Salmon E, Perani D, Kessler J, Mielke R et al (1999). Impairment of neocortical metabolism predicts progression in Alzheimer's disease. *Dement Geriatr Cogn Disord* **10**: 494–504.
- Herholz K, Salmon E, Perani D, Baron JC, Holthoff V, Frolich L et al (2002). Discrimination between Alzheimer dementia and controls by automated analysis of multicenter FDG PET. *Neuroimage* **17**: 302–316.
- Hixson JE, Powers PK (1991). Restriction isotyping of human apolipoprotein A—IV: rapid typing of known isoforms and detection of a new isoform that deletes a conserved repeat. *J Lipid Res* **32**: 1529–1535.
- Hoffman JM, Welsh-Bohmer KA, Hanson M, Crain B, Hulette C, Earl N et al (2000). FDG PET imaging in patients with pathologically verified dementia. *J Nucl Med* **41**: 1920–1928.
- Horwitz B, McIntosh AR, Haxby JV, Grady CL (1995). Network analysis of brain cognitive function using metabolic and blood flow data. *Behav Brain Res* **66**: 187–193.
- Huang C, Wahlund LO, Svensson L, Winblad B, Julin P (2002). Cingulate cortex hypoperfusion predicts Alzheimer's disease in mild cognitive impairment. *BMC Neurol* **2**: 9–16.
- Ishii K, Sasaki M, Yamaji S, Sakamoto S, Kitagaki H, Mori E (1997). Demonstration of decreased posterior cingulate perfusion in mild Alzheimer's disease by means of H₂¹⁵O positron emission tomography. *Eur J Nucl Med* **24**: 670–673.
- Jacobs DM, Sano M, Dooneief G, Marker K, Bell KL, Stern Y (1995). Neuropsychological detection and characterization of preclinical Alzheimer's disease. *Neurology* **45**: 957–962.
- Johnson KA, Jones K, Holman BL, Becker JA, Spiers PA, Satlin A (1998). Preclinical prediction of Alzheimer's disease using SPECT. *Neurology* **50**: 1563–1571.
- Liang KY, Zeger SL (1986). Longitudinal data analysis using generalized linear models. *Biometrika* **73**: 13–22.
- McKhann G, Drachman D, Folstein M, Katzman R, Price D, Stadlan EM (1984). Clinical diagnosis of Alzheimer's disease: report of the NINCDS-ADRDA Work Group under the auspices of Department of Health and Human Services Task Force on Alzheimer's Disease. *Neurology* **34**: 939–944.
- Meltzer CC, Zubietta JK, Brandt J, Tune LE, Mayberg HS, Frost JJ (1996). Regional hypometabolism in Alzheimer's disease as measured by positron emission tomography after correction for effects of partial volume averaging. *Neurology* **47**: 454–461.
- Millien I, Blaizot X, Giffard C, Mezenge F, Insausti R, Baron JC et al (2002). Brain glucose hypometabolism after perirhinal lesions in baboons: implications for Alzheimer disease and aging. *J Cereb Blood Flow Metab* **22**: 1248–1261.
- Minoshima S, Giordani B, Berent S, Frey KA, Foster NL, Kuhl DE (1997). Metabolic reduction in the posterior cingulate cortex in very early Alzheimer's disease. *Ann Neurol* **42**: 85–94.
- Mintun MA, Lundstrom BN, Snyder AZ, Vlassenko AG, Shulman GL, Raichle ME. (2001). Blood flow and oxygen delivery to human brain during functional activity: theoretical modeling and experimental data. *Proc Natl Acad Sci USA* **98**: 6859–6864.
- Moeller JR, Strother SC, Sidtis JJ, Rottenberg DA (1987). Scaled subprofile model: a statistical approach to the analysis of functional patterns in positron emission tomographic data. *J Cereb Blood Flow Metab* **7**: 649–658.
- Mosconi L, Tsui WH, De Santi S, Li J, Rusinek H, Convit A et al (2005). Reduced hippocampal metabolism in MCI and AD: automated FDG-PET image analysis. *Neurology* **64**: 1860–1867.
- Press DZ, Casement M, Alsup D (2003). Hippocampal formation hyperperfusion in early Alzheimer's disease. *Neurology* **60**(Suppl 1): A113.
- Reiman EM, Caselli RJ, Yun LS, Chen K, Bandy D, Minoshima S et al (1996). Preclinical evidence of Alzheimer's disease in persons homozygous for the epsilon 4 allele for apolipoprotein E. *N Engl J Med* **334**: 752–758.
- Scarmeas N, Habeck CG, Zarahn E, Anderson KE, Park A, Hilton J et al (2004). Covariance PET patterns in early Alzheimer's disease and subjects with cognitive impairment but no dementia: utility in group discrimination and correlations with functional performance. *Neuroimage* **23**: 35–45.
- Silverman DH, Cummings JL, Small GW, Gambhir SS, Chen W, Czernin J et al (2002). Added clinical benefit of incorporating 2-deoxy-2-[18F]fluoro-D-glucose with positron emission tomography into the clinical evaluation of patients with cognitive impairment. *Mol Imaging Biol* **4**: 283–293.
- Silverman DH, Small GW, Chang CY, Lu CS, Kung De Aburto MA, Chen W et al (2001). Positron emission tomography in evaluation of dementia: regional brain metabolism and long-term outcome. *JAMA* **286**: 2120–2127.
- Small GW, Mazziotta JC, Collins MT, Baxter LR, Phelps ME, Mandelkern MA et al (1995). Apolipoprotein E type 4 allele and cerebral glucose metabolism in relatives at risk for familial Alzheimer disease. *JAMA* **273**: 942–947.
- Stern Y, Moeller JR, Anderson KE, Luber B, Zubin NR, DiMauro AA et al (2000). Different brain networks mediate task performance in normal aging and AD: defining compensation. *Neurology* **55**: 1291–1297.
- Su PC, Ma Y, Fukuda M, Mentis MJ, Tseng HM, Yen RF et al (2001). Metabolic changes following subthalamotomy for advanced Parkinson's disease. *Ann Neurol* **50**: 514–520.

- Tabert MH, Albert SM, Borukhova-Milov L, Camacho Y, Pelton G, Liu X *et al* (2002). Functional deficits in patients with mild cognitive impairment: prediction of AD. *Neurology* **58**: 758–764.
- Tanna NK, Kohn MI, Horwich DN, Jolles PR, Zimmerman RA, Alves WM *et al* (1991). Analysis of brain and cerebrospinal fluid volumes with MR imaging: impact on PET data correction for atrophy. Part II. Aging and Alzheimer dementia. *Radiology* **178**: 123–130.
- Wu HM, Bergsneider M, Glenn TC, Yeh E, Hovda DA, Phelps ME *et al* (2003). Measurement of the global lumped constant for 2-deoxy-2-[18F]fluoro-D-glucose in normal human brain using [15O]water and 2-deoxy-2-[18F]fluoro-D-glucose positron emission tomography imaging. A method with validation based on multiple methodologies. *Mol Imaging Biol* **5**: 32–41.